Analyzing the Theoretical Limits of Forced Air-Cooling by Employing Advanced Composite Materials with Thermal Conductivities > 400W/mK

Uwe DROFENIK and Johann W. KOLAR

Power Electronic Systems Laboratory, ETH Zurich
ETH-Zentrum / ETL H13, CH-8092 Zurich, Switzerland
Phone: +41-44-632-4267, Fax: +41-44-632-1212, E-mail: drofenik@lem.ee.ethz.ch

Abstract

The cooling system takes a significant portion of the total mass and/or volume of a power electronic system. In order to design a converter with high power density, it is necessary to minimize the converter's cooling system volume for a given maximum tolerable thermal resistance. This paper theoretically investigates, if the cooling system volume can be significantly reduced by employing new advanced composite materials like isotropic Aluminum/Diamond Composites or anisotropic Highly Orientated Pyrolytic Graphite (HOPG). Another strategy to improve the power density of the cooling system is to increase the rotating speed and/or the diameter of the fan, which is limited by increasing power consumption of the fan. Fan scaling laws are employed in order to describe volume and thermal resistance of an optimized cooling system (fan plus heat sink), resulting in a single compact equation dependent on just two design parameters. Based on this equation, a deep insight into different design strategies and their general potentials is possible. The theory of the design process is verified experimentally for cooling a 10kW-converter.

1. Introduction

Power electronic converters are essential system components wherever electricity has to be provided. There is a strong desire to continuously increase the power density of converter systems to ease their integration into larger systems and products. Since the cooling system of a converter is typically a significant contributor to its volume and weight, therefore, in this paper we investigate the theoretical limits of minimizing the volume of a forced air convective cooling system composed of fan and heat sink for a desired thermal resistance.

Material	Thermal Conduct. [W/mK]	In-plane CTE [ppm/K]	Specific weight [kg/m^3]
Aluminum	210 (isotr.)	23	2700
Copper	380 (isotr.)	17	8930
Diamond	2200 (isotr.)	2	3500
Natural Graphite in Epoxy-Matrix	370 (xy) / 6.5 (z-dir.)	-2.4	1940
Continuous Carbon Fibers in SiC-Matrix	370 (xy) / 38 (z-dir.)	2.5	2200
Diamond Particles in Al-Matrix	650 (isotr.)	7	3100
Highly Orientated Pyrolytic Graphite	1700 (xy) / 20 (z-dir.)	8	2250

Tab.1: Properties of thermal materials ([1] – [6]).

A very interesting development is the recent introduction of new materials providing extremely high thermal conductivity (**Tab.1**), that theoretically might be employed as heat sink material. Alternatively and/or additionally the fan power could be increased in order to improve the convective cooling. In the following, we investigate if it makes sense to consider employing such advanced materials as heat sink material, and what performance improvements might be possible. The question of manufacturing such heat sinks and fans, of their reliable operation and of the costs is excluded in this first study. Although this investigation is mainly theoretical, we discuss practical aspects in section 3, and give experimental data of prototype heat sinks optimized according to the theory presented here in order to verify our underlying mathematical models.

Basically, the optimization can be explained like this: For a heat sink channel with a certain length in air flow direction, there results a certain pressure drop along the channel. Balancing this pressure drop against the fan pressure gives the operating point of the fan. Increasing the length of the heat sink will increase the pressure drop and reduce the air flow volume, but on the other hand increase the total fin surface employed for convective cooling. Here, an optimum heat sink length concerning minimum thermal resistance of the heat sink can be found. An important side condition is the minimum base plate area A_{CHIP} needed for placing the power chips of the converter. For each fin there is a certain minimum thickness necessary to transport an optimum amount of heat to the fin surface. If the thermal conductivity of the fin material is increased, thinner fins can be employed, which means that the number of fins can be increased resulting in a larger total fin surface, and, therefore, improved convective heat transfer ([7], [8]). Since all these effects are highly non-linear, we cannot simply assume that, e.g., doubling the thermal conductivity of the material will reduce the thermal resistance of the heat sink by a factor of two. It is necessary, to perform an analytical description of this heat transfer problem based on empirical expressions, and then to perform a systematic optimization.

2. Optimization of Cooling System Design

2.1 Detailed Optimization Procedure

Based on empirical and analytical expressions, the air flow and the resulting thermal resistance of the heat sink can be calculated as performed in the following. A detailed description of the mathematical procedure and

the equations (1) – (14), and the accuracy of the theory verified by experimental results, can be found in [8] – [10]. The investigation is limited to the heat sink shape shown in **Fig.1**.

k	fin spacing ratio
λ_{HS} *[W/mK]*	thermal conductivity of heat sink material
A_{HS} *[m²]*	size of the heat sink base plate
d_h *[m]*	hydraulic diameter of one channel
L *[m]*	channel length in air flow direction
n	number of channels
Δp *[N/m²]*	pressure drop in one channel
V *[m³/s]*	volume flow
Re_m	avg. Reynolds number (for lam. or turb. flow)
Nu_m	avg. Nusselt number (for lam. or turb. flow)
h *[W/m²K]*	(convective) heat transfer coefficient
$Pr \approx 0.71$	Prandtl number (air, 80°C)
$\rho_{AIR} \approx 0.99$ *[kg/m³]*	air density (80°C)
$\nu_{AIR} \approx 2.1\text{e-}5$ *[m²/s]*	cinematic viscosity of the air (80°C)
$c_{p,AIR} \approx 1010$ *[J/kgK]*	specific thermal capacitance of air
$\lambda_{AIR} \approx 0.03$ *[W/mK]*	thermal conductivity of air (80°C)

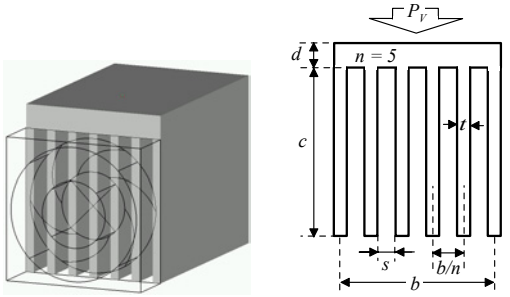

Fig.1: Geometry of the heat sink investigated in this paper. In order to provide the whole fin surface with air flow, the heat sink dimensions have to match the fan size resulting in $b = c = D$, where D is the diameter of the fan facing the heat sink. Thermal losses P_V *[W]* occur at the top of the base plate and are homogenously distributed over the area $A_{CHIP} = b \cdot L$.

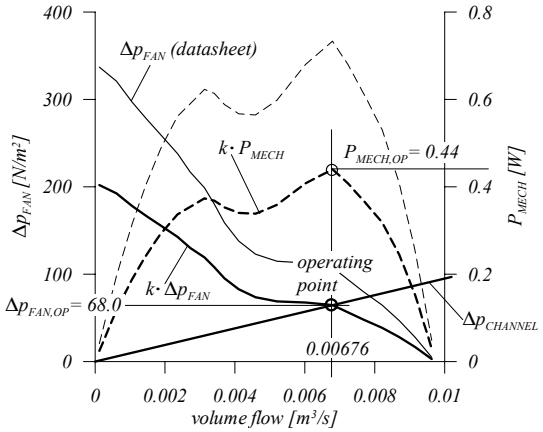

Fig.2: Fan characteristic of SunAce 40x40x28/50dB [11] showing fan pressure Δp_{FAN} dependent on the air flow V *[m³/s]*. To calculate the fan operating point, Δp_{FAN} has to be multiplied with the fin spacing ration k. The heat sink channel pressure drop $\Delta p_{CHANNEL}$ is shown for laminar flow in linear dependency of the flow. Intersection of the two characteristics gives the fan operating point which is for optimized heat sinks typically (but not necessarily!) close to the maximum "mechanical power" of the air flow.

$$k = \frac{s}{b/n} \tag{1}$$

$$d_h = \frac{2s \cdot c}{s + c} \tag{2}$$

$$\Delta p_{lam}(V) = \frac{48\ \rho_{AIR}\ \nu_{AIR}\ L}{n\,(s \cdot c)\,d_h^2}\ V \tag{3}$$

$$\Delta p_{turb}(V) = \frac{L\,\frac{s+c}{2s \cdot c}\,\rho_{AIR}\,\frac{1}{2}\left(\frac{V}{n(s \cdot c)}\right)^2}{\left(0.79 \cdot \ln\left(\frac{2V}{n\,(s+c)\nu_{AIR}}\right) - 1.64\right)^2} \tag{4}$$

$$Re_m = \frac{2V}{n(s+c)\nu_{AIR}} \tag{5}$$

$$k \cdot \Delta p_{FAN}(V) = \Delta p_{lam}(V_{lam}) \rightarrow V_{lam} \rightarrow Re_{m,lam} < 2300\,? \tag{6}$$

$$Nu_{m,lam} = \frac{3.657\left[\tanh\left(2.264X^{1/3} + 1.7X^{2/3}\right)\right]^{-1} + \frac{0.0499}{X}\tanh(X)}{\tanh\left[2.432\ Pr^{1/6}X^{1/6}\right]} \tag{7}$$

$$X = \frac{L}{d_h\,Re_m\,Pr} \tag{8}$$

$$Nu_{m,turb} = \frac{\left\{8 \cdot (0.79 \cdot \ln(Re_m) - 1.64)^2\right\}^{-1}(Re_m - 1000)\ Pr}{1 + 12.7\sqrt{\left\{8 \cdot (0.79 \cdot \ln(Re_m) - 1.64)^2\right\}^{-1}}\,(Pr^{2/3} - 1)} \cdot \left(1 + \left(\frac{d_h}{L}\right)^{2/3}\right) \tag{9}$$

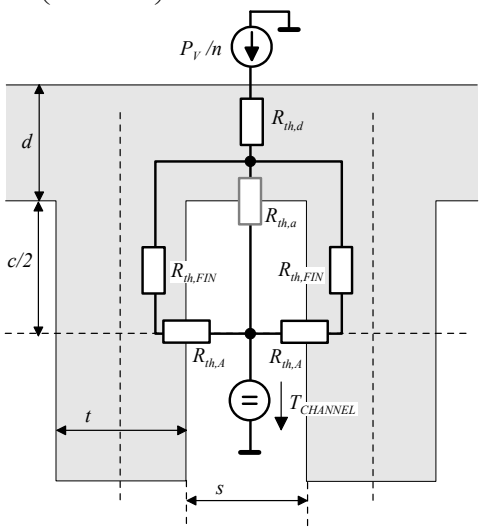

Fig.3: Thermal network to describe the heat transfer from heat sink surface (location of the chips) into the air, which is flowing through a channel of the heat sink.

The procedure of obtaining the pressure in one channel ((3) – (6)) is shown graphically in **Fig.2**. Employing (6), it is decided if the flow problem is laminar or turbulent. With empirical equations (7) – (9) the convective heat transfer is defined. Finally, employing the model of **Fig.3**, the thermal resistance of the heat sink can be calculated via (10) – (14). The non-linear equations (1) – (14) can be easily solved numerically [8], but due to their complexity, it is very difficult to gain insight into the relationships between various design parameters like fan speed, fan diameter, thermal conductivity of the heat sink material, total chip area or heat sink length.

$$h = \frac{Nu_m \cdot \lambda_{AIR}}{d_h} \tag{10}$$

$$R_{th,A} = \frac{1}{h \cdot L \cdot c} \tag{11}$$

$$R_{th,FIN} = \frac{\frac{1}{2}c}{\frac{1}{2}t \cdot L \cdot \lambda_{HS}} \tag{12}$$

$$R_{th,d} = \frac{d}{\frac{1}{n} A_{HS} \lambda_{HS}} \tag{13}$$

$$R_{th,S-a}^{(HS)} = \tfrac{1}{n}(R_{th,d} + \tfrac{1}{2}(R_{th,FIN} + R_{th,A})) + \frac{0.5}{\rho_{AIR}\, c_{P,AIR}\, V} \tag{14}$$

2.2 Analyzing the Different Contributions to the Thermal Resistance of the Heat Sink

With some general assumptions, equations (1) – (14) can be significantly simplified. The simplified equations as presented in the following, are not useful to meet specific design targets like a certain $R_{th,S\text{-}a}^{(HS)}$ with very high accuracy, but clearly show what kind of design parameters influence the system on what scale. The merit of certain optimization strategies like increasing the fan rotating speed, changing the geometric design of the heat sink or increasing the thermal conductivity of the heat sink material, can be seen much more clearly.

The first assumption for deriving the simplified equations is, that we operate the fan close to the maximum mechanical power, and that $\Delta p_{F,MAX}$ is reduced by approximately 50% (factor *0.5* in (16)) due to the partial air flow from the fan facing not channels but fins [9]. Because for typical fans the maximum mechanical power is shifted from the symmetric center to the right (see Fig.2), we can write in a rough approximation

$$V_{MAX} \approx \tfrac{2}{3} V_{F,MAX} \tag{15}$$

$$\Delta p_{MAX} \approx \tfrac{1}{3} \cdot 0.5\, \Delta p_{F,MAX} \tag{16}$$

This is also a fan operating area that is often recommended in fan datasheets. Our second assumption is that the number of fins is larger than at least 5, so that we can write

$$s << c \quad \rightarrow \quad d_h \approx 2s \tag{17}$$

The third assumption is laminar or mixed flow in the operating point. As we experienced in various optimizations [8], the optimized operating point is very often in the vicinity of the boundary region between laminar and turbulent flow ("mixed flow"), where the laminar equations are still valid in very good approximation. From (3) we get

$$\frac{s^3 n\, c}{L} = 48 \cdot \rho_{AIR} \nu_{AIR} \frac{V_{F,MAX}}{\Delta p_{F,MAX}} \approx 10^{-3} \frac{V_{F,MAX}}{\Delta p_{F,MAX}} \tag{18}$$

which defines the condition to operate the fan close to its maximum mechanical power. Then, the fin thickness can be calculated as

$$t = \frac{c}{n} - s \approx s \cdot \left[10^3 \frac{\Delta p_{F,MAX}}{V_{F,MAX}} \frac{s^2 c^2}{L} - 1 \right] \tag{19}$$

which must not be negative, resulting in the condition

$$s > \sqrt{10^{-3} \frac{V_{F,MAX}}{\Delta p_{F,MAX}} \frac{L}{c^2}} \tag{20}$$

In (17) we assume a minimum fin number of 5, resulting in the second condition for the channel thickness s as

$$n = 10^{-3} \frac{V_{F,MAX}}{\Delta p_{F,MAX}} \frac{L}{s^3 c} \geq 5 \;\rightarrow\; s \leq \sqrt[3]{\tfrac{1}{5} \cdot 10^{-3} \frac{V_{F,MAX}}{\Delta p_{F,MAX}} \frac{L}{c}} \tag{21}$$

As can be seen in (14), the thermal resistance of the heat sink $R_{th,S\text{-}a}^{(HS)}$ is composed of three components: The conductive resistance of the sink material $R_{th,FIN}^{*}$ mainly through the fins, a convective resistance $R_{th,conv}$ from fin surface into the air, and a resistance $R_{th,\Delta T}$ due to the temperature rise of the air flowing from channel inlet to channel outlet.

$$R_{th,S-a}^{(HS)} = R^{*}_{th,FIN} + R_{th,conv} + R_{th,\Delta T} \tag{22}$$

$$R^{*}_{th,FIN} = \tfrac{1}{n} R_{th,d} + \tfrac{1}{2n} R_{th,FIN} \approx \tfrac{1}{2n} R_{th,FIN} = \frac{c}{2n\, \lambda_{HS} L t} = \frac{1}{2\lambda_{HS} L} \cdot \frac{1}{1 - 10^{-3} \frac{V_{F,MAX}}{\Delta p_{F,MAX}} \frac{L}{s^2 c^2}} \tag{23}$$

The equation of the laminar Nusselt number (7) can be approximated as

$$Nu_{m,lam} \approx 2.7 \cdot \left[1 + \frac{1}{4.5\sqrt{X}} \right] \tag{24}$$

with

$$X \approx \frac{3 \nu_{AIR}}{8\, Pr} \cdot \frac{L\, n\, c}{V_{F,MAX}} \tag{25}$$

resulting in

$$Nu_{m,lam} \approx 2.7 \cdot \left[1 + 66.7 \cdot \sqrt{V_{F,MAX} \frac{s}{L\, n\, c}} \right] \tag{26}$$

Based on this and employing (11), (17) and (18), the convective resistance is given as

$$R_{th,conv} = \tfrac{1}{2n} \frac{2s}{L\, c\, \lambda_{AIR} Nu_{m,lam}} \approx \frac{1.3 \cdot 10^4 \frac{\Delta p_{F,MAX}}{V_{F,MAX}} \frac{s^4}{L^2}}{1 + 2 \cdot 10^3 \cdot \sqrt{\Delta p_{F,MAX}} \cdot \frac{s^2}{L}} \tag{27}$$

Finally, the third resistive component is calculated as

$$R_{th,\Delta T} = \frac{0.5}{\rho_{AIR}\, c_{p,AIR} \cdot \frac{2}{3} V_{F,MAX}} \approx \frac{7.5 \cdot 10^{-4}}{V_{F,MAX}} \tag{28}$$

2.3 Influence of the Fan

Maximum air flow rate $V_{FAN,MAX}$ *[m³/s]*, pressure $\Delta p_{FAN,MAX}$ *[N/m²]*, input power P_{FAN} *[W]* and noise $noise_{FAN}$ *[dB]* of a fan are dependent [12] on rotating speed N *[rmp]* and diameter D *[m]* as described by

$$V_{F,MAX} = k_1 \cdot N \cdot D^3 \tag{29}$$

$$\Delta p_{F,MAX} = k_2 \cdot N^2 \cdot D^2 \tag{30}$$

$$P_{FAN} = k_3 \cdot N^3 \cdot D^5 \tag{31}$$

$$noise_{FAN} \propto \log(N) \tag{32}$$

Based on datasheet information [11], we investigated 65 commercially available fans for electronics cooling. The fan diameters varied from *40mm* to *200mm* (factor *5*), the rated power varied between *0.5W* and *25W* (factor *50*), the rated fan speed between *1,700rpm* and *15,500rpm* (variation factor *9*). Using the simple laws (29) – (31), we calculated the parameters k_1, k_2, k_3 for these 65 fans as

$$k_1 = \left[6.0 \cdot 10^{-3} \ldots 13.5 \cdot 10^{-3} \right] \tag{33}$$

$$k_2 = \left[3.94 \cdot 10^{-4} \ldots 8.85 \cdot 10^{-4} \right] \tag{34}$$

$$k_3 = \left[3.0 \cdot 10^{-6} \ldots 76.5 \cdot 10^{-6} \right] \tag{35}$$

The parameters k_1 and k_2 remain within a comparably small range. The variations in (33) and (34) can be explained by variations of about a factor *2* of the ratio of fan height and fan diameter for different investigated types. The wide variation of k_3 in (35) is due to the

mechanical efficiency of the fan: The minimum gap width between fan blade and housing is limited by manufacturing tolerances. With decreasing fan diameter D, the ratio of this gap (where the turbulent losses occur) and the diameter increases in a non-linear way. This results in a non-linear decrease of fan efficiency, and in very large values of k_3 for small fan diameters as compared to larger ones. With the fan laws (29) – (31), assuming $D = c$, and defining

$$A_1 = 10^{-3}\,\tfrac{k1}{k2} \qquad A_2 = 5\cdot 10^{-4}\,\tfrac{1}{\sqrt{k2}} \qquad A_3 = 6.5\,\tfrac{\sqrt{k2}}{k1} \qquad A_4 = 7.5\cdot 10^{-4}\,\tfrac{1}{k1} \tag{36}$$

the three thermal resistance components of the heat sink can be written as

$$R^*_{th,FIN} = \frac{\frac{1}{2\lambda_{HS} L}}{1-10^{-3}\,\frac{k1}{k2}\frac{L}{N s^2 c}} = \frac{\frac{1}{2\lambda_{HS} L}}{1-A_1\cdot\frac{L}{N s^2 c}} \tag{37}$$

$$R_{th,conv} = \frac{1.3\cdot 10^4\,\frac{k2}{k1}\frac{s^4}{L^2 c}}{\frac{1}{N}+2\cdot 10^3\cdot\sqrt{k_2}\cdot\frac{s^2 c}{L}} = \frac{A_3\cdot\frac{s^2}{L\,c^2}}{1+A_2\cdot\frac{L}{N s^2 c}} \tag{38}$$

$$R_{th,\Delta T} = \frac{7.5\cdot 10^{-4}}{k_1}\cdot\frac{1}{N c^3} = \frac{A_4}{N c^3} \tag{39}$$

2.4 Optimizing the Cooling System Performance Index (CSPI)

The power density d_{SYS} *[kW/liter]* of the converter system is defined as

$$d_{SYS} = \frac{P_{OUT,SYS}}{Vol_{SYS}} = \frac{\eta_{SYS}}{1-\eta_{SYS}}\frac{P_{V,SYS}}{Vol_{SYS}} = \frac{\eta_{SYS}}{1-\eta_{SYS}}\frac{\Delta T^{max}_{S-a}}{R_{th,S-a}\,Vol_{SYS}} \tag{40}$$

For comparison of different heat sink designs concerning power density, we proposed in [8] the "cooling system performance index (CSPI)" (see also [13], published at the same time, and giving results in good agreement with the findings of this study), as

$$CSPI\left[\tfrac{W}{K\cdot liter}\right] = \frac{1}{R_{th,S-a}\left[\tfrac{K}{W}\right]\cdot Vol_{CS}[liter]} \tag{41}$$

The cooling system power density d_{CS} *[W/liter]* can be expressed proportional to *CSPI* as

$$d_{CS}\left[\tfrac{W}{liter}\right] = \frac{P_{OUT,SYS}}{Vol_{CS}} = \frac{\eta_{SYS}}{1-\eta_{SYS}}\,\Delta T^{max}_{S-a}\cdot CSPI \quad > d_{SYS} \tag{42}$$

The density d_{CS} considers all components of the cooling system. In case of forced air-cooling this is the heat sink volume plus the fan volume.

The CSPI is very useful to directly compare heat sink plus fan combinations of different size, of different types and in different applications. If an approximate value of CSPI is known, and the maximum allowed thermal resistance of the heat sink is given (from the knowledge of maximum ambient temperature, maximum junction temperature and maximum semiconductor junction-to-case temperature), the volume of the cooling system of the converter can be directly calculated. This makes it very easy for the electrical engineer to roughly estimate the total volume, mass and power density of a converter design without any deeper knowledge of the cooling system. For commercial non-optimized heat sinks for converter systems in the kW-range employing forced air-cooling, the value of CSPI is typically in the range of *3* to *5* (as shown in [8]). Optimized heat sinks can reach much higher CSPI-values as shown in the following.

Defining the total chip area to be cooled as

$$A_{CHIP} = L\,c \tag{43}$$

we can, based on the assumption that the fan thickness is approximately one third of its diameter, define

$$CSPI^{-1} = R^{(HS)}_{th,S-a}\cdot Vol_{CS} = (R^*_{th,FIN} + R_{th,conv} + R_{th,\Delta T})\cdot(L+\tfrac{1}{3}c)\,c^2 = \\ = CSPI^{-1}_{FIN} + CSPI^{-1}_{conv} + CSPI^{-1}_{\Delta T} \tag{44}$$

assuming that the gap between fan and heat sink is small compared to c and L. This gives the inverse of CSPI as

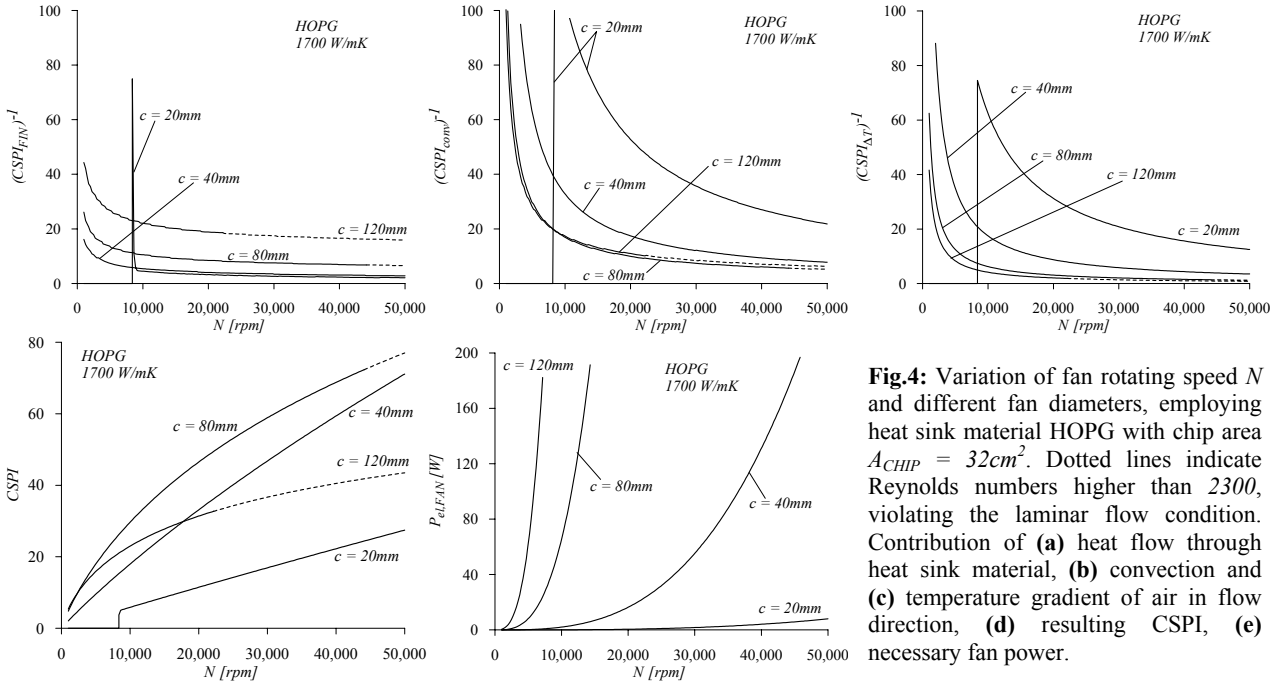

Fig.4: Variation of fan rotating speed N and different fan diameters, employing heat sink material HOPG with chip area A_{CHIP} = *32cm²*. Dotted lines indicate Reynolds numbers higher than *2300*, violating the laminar flow condition. Contribution of **(a)** heat flow through heat sink material, **(b)** convection and **(c)** temperature gradient of air in flow direction, **(d)** resulting CSPI, **(e)** necessary fan power.

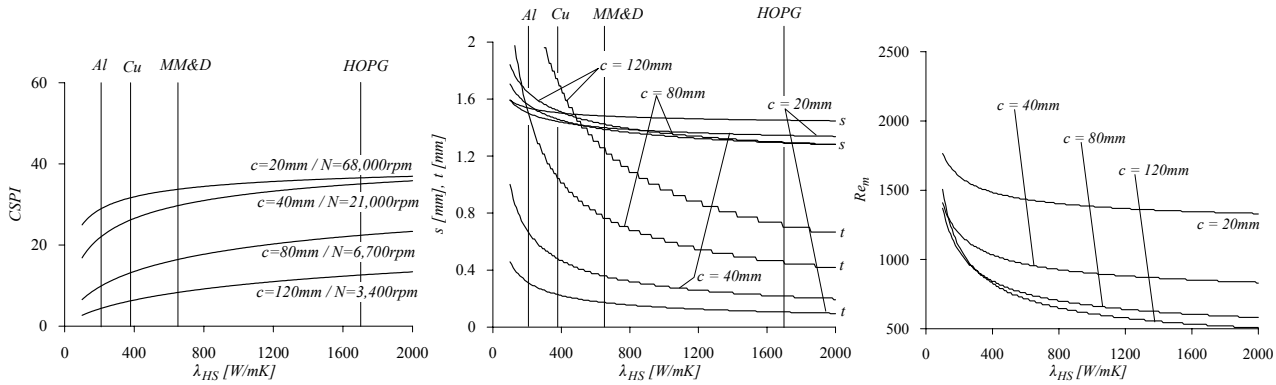

Fig.5: Variation of thermal conductivity of heat sink material λ_{HS} with $P_{FAN,MAX} = 20W$ and $A_{CHIP} = 32cm^2$.

$$CSPI^{-1} = \frac{\frac{c^2}{2\lambda_{HS}}\left(1+\frac{c^2}{3A_{CHIP}}\right)}{1-A_1\cdot\frac{A_{CHIP}}{N s^2 c^2}} + \frac{A_3\cdot\left(1+\frac{c^2}{3A_{CHIP}}\right)s^2}{1+A_2\cdot\frac{A_{CHIP}}{N s^2 c^2}} + \frac{A_4\cdot\left(\frac{A_{CHIP}}{c^2}+\frac{1}{3}\right)}{N} \quad (45)$$

with the necessary side condition (see (20) and (21))

$$\sqrt{A_1\cdot\frac{A_{CHIP}}{N c^2}} \le s \le \sqrt[3]{\frac{A_1}{5}\cdot\frac{A_{CHIP}}{N c}} \quad (46)$$

The fin number is

$$n = (\text{int})\left[A_1\cdot\frac{A_{CHIP}}{N s^3 c}\right] \quad (47)$$

and the Reynolds number

$$Re_m = 6.35\cdot10^4\cdot k_1\cdot\frac{N c^2}{n} \quad (48)$$

must not be significantly larger than *2300* in order to verify the original assumption of laminar or mixed flow in the heat sink channels [10]. For optimization of the CSPI, the optimum channel width has to be found for every parameter set (λ_{HS}, A_{CHIP}, c, N).

Fan rotating speed dependency of the three terms in (45) contributing to the total CSPI are shown in **Fig.4** for heat sink material HOPG. Only the term $(CSPI_{FIN})^{-1}$ (Fig.4(a)) can be influenced by the heat sink conductivity. Therefore, it only makes sense to invest in advanced materials, if the other two terms $(CSPI_{conv})^{-1}$ (Fig.4(b)) and $(CSPI_{\Delta T})^{-1}$ (Fig.4(c)) are small compared to $(CSPI_{FIN})^{-1}$. For small rotating speed N and small diameter c, the term $(CSPI_{FIN})^{-1}$ will be negative which means there is no design solution with an operating point as defined in (15) and (16). In this example, the chip area A_{CHIP} is set to be $32cm^2$ which is approximately the space needed for all three power modules containing the chips for a 10kW Vienna Rectifier (VR1).

Theoretically, as shown in Fig.4(d), there is no limit of the CSPI if the fan rotating speed N is increased. But, as one can immediately see from Fig.4(e), the power consumption of the fan will reach unrealistic high values. Therefore, by defining the maximum acceptable power consumption $P_{FAN,MAX}$ from (31), the maximum tolerated fan rotating speed can be expressed in terms of the fan diameter $D = c$ as

$$N = \sqrt[3]{\frac{1}{k_3}\cdot P_{FAN}^{\max}}\cdot c^{-5/3} \quad (49)$$

resulting in

$$CSPI^{-1} = CSPI^{-1}(c,\lambda_{HS},A_{CHIP},P_{FAN}^{\max}) = Rth_{S-a}^{HS}\cdot Vol_{CS} = \quad (50)$$
$$\frac{\frac{c^2}{2\lambda_{HS}}\left(1+\frac{c^2}{3A_{CHIP}}\right)}{1-\frac{A_1\cdot A_{CHIP}}{s^2\cdot\sqrt[3]{\frac{1}{k_3}\cdot P_{FAN}^{\max}}\cdot c^{1/3}}} + \frac{A_3\cdot\left(1+\frac{c^2}{3A_{CHIP}}\right)s^2}{1+\frac{A_2\cdot A_{CHIP}}{s^2\cdot\sqrt[3]{\frac{1}{k_3}\cdot P_{FAN}^{\max}}\cdot c^{1/3}}} + \frac{A_4\cdot\left(A_{CHIP}+\frac{1}{3}c^2\right)}{\sqrt[3]{\frac{1}{k_3}\cdot P_{FAN}^{\max}}\cdot c^{1/3}}$$

which is dependent only on the thermal conductivity of the heat sink λ_{HS} and the diameter of the fan c. The channel width s has to be always chosen in order to maximize CSPI. Therefore, the channel width s is not an independent design parameter in this equation. Condition (46) has to be fulfilled, and (48) should not be violated.

In **Fig.5** the results of the numerical computation of (50) is shown. The chip area A_{CHIP} is selected to fulfill the specifications of a 10kW Vienna Rectifier (VR1), and the fan losses are limited to *20W*. Fig.5(a) shows that with increasing λ_{HS} the CSPI becomes flat because only the first term $(CSPI_{FIN})^{-1}$ is affected. Fig.5(b) shows the fin and channel geometry necessary to realize the optimum heat sink. With larger values of λ_{HS} the fin thickness must be manufactured below *0.5mm* which provides a limit to the practical realization as also discussed in section 3. Fig.5(c) shows that the Reynolds number is always below *2300*.

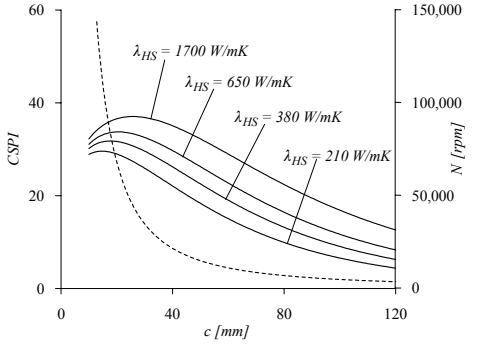

Fig.6: Variation of c with $A_{CHIP}=32cm^2$ and $P_{FAN,MAX}=20W$.

In **Fig.6** (all parameters equal to Fig.5) fan diameter c is varied. From Fig.5 and Fig.6 one can see, that it is possible for cooling systems of converters in the kW-range to reach a CSPI of about *20* (*5* times larger than typical commercial heat sinks) by employing aluminum and optimizing fan and heat sink geometry. Employing materials with much higher thermal conductivities does not improve the CSPI significantly.

3. Practical Considerations

In the previous theoretical sections we did not comment on the many practical difficulties associated with the materials shown in Tab.1. To name a few well-known problems, HOPG shows only high thermal conductivity in-plane which is sufficient for the fins but provides very poor heat spreading within the base plate. HOPG is very expensive – according to [6], the material for a prototype as shown in **Fig.7** would cost more than 1000 Euro. Employing Al-diamond metal-matrix [4], [5] might limit the fin thickness minimum to about *1.0mm* which is far above the calculated optimum (Fig.5(b)). Also, efficient manufacturing procedures are still under investigation.

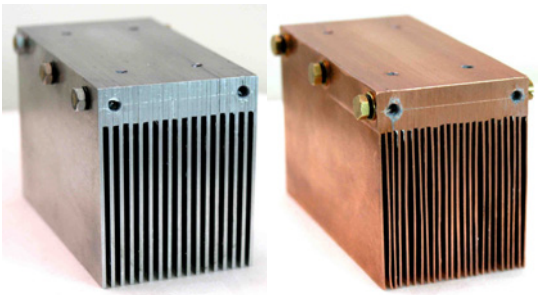

Fig.7: Optimized heat sink employing SanAce 40x40x28mm/50dB [11] with $b=c=40mm$, $d=10mm$, $L=80mm$, $A_{CHIP}= 32cm^2$, $Vol_{CS}=0.22\ liter$. **(a)** Aluminum with $n=16$, $s=1.5mm$, $t=1.0mm$ **(b)** Copper with $n=23$, $s=1.3mm$, $t=0.5mm$.

Two optimized heat sinks for a 10kW-VR1 based on (1) – (14) and/or (50) are shown in Fig.7. Details of manufacturing, measurements and design tolerances will soon be published. The measurements verify the theoretical calculations with very good accuracy. For Fig.7(a), aluminum, we measured $R_{th}=0.260$ (theory: $R_{th}=0.254$) and $CSPI=17.5$ (theory: $CSPI=20.0$), and for Fig.7(b), copper, we measured $R_{th}=0.215$ (theory: $R_{th}=0.240$) and $CSPI=21.1$ (theory: $CSPI=22.2$).

4. Alternative Designs for Future Research

The main limitation of the optimization procedure is, according to the shape shown in Fig.1, the strict coupling between fan diameter and fin height ($D = c$). By choosing different cooling system designs, this coupling of fan characteristic and heat sink geometry is partly eliminated, and improvement of the CSPI might be possible. Design proposals providing such possible decoupling are shown in **Fig.8**, which will be the topic of future research.

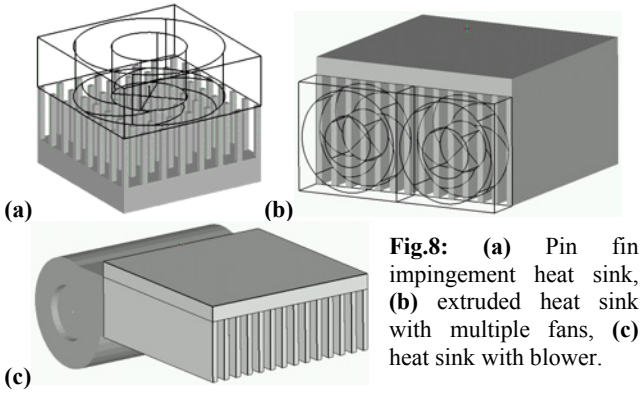

Fig.8: **(a)** Pin fin impingement heat sink, **(b)** extruded heat sink with multiple fans, **(c)** heat sink with blower.

5. Conclusion

We gave an equation to directly calculate the Cooling System Performance Index (CSPI) that specifies cooling system volume for a given thermal resistance, by taking into account thermal conductivity of the heat sink material and fan characteristic. An optimization for a 10kW converter shows that aluminum might still be a very good choice considering manufacturability, weight and cost (**Fig.9**). But for different applications and/or design specifications advanced thermal materials might provide enormous potential for cooling power electronics.

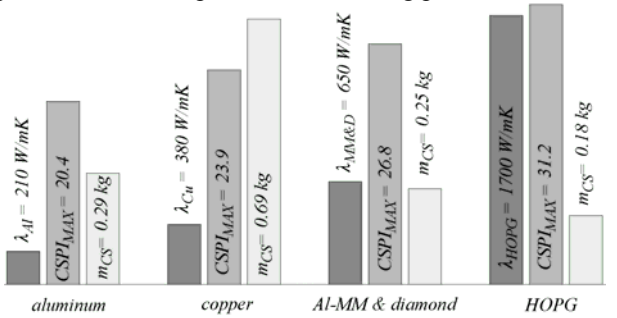

Fig.9: Comparing different heat sink materials for a 10kW-VR1.

Literature

[1] C. Zweben, "'Revolutionary' New Thermal Management Materials, Electronics Cooling", vol.11, no2, pp. 36-37, May 2005

[2] C. Zweben, "Ultrahigh-thermal-conductivity packaging materials", 21st Annual IEEE Semiconductor Thermal Measurement and Management Symposium, 15-17 March 2005, pp. 168 - 174

[3] C. Zweben, "Advanced composites and other advanced materials for electronic packaging thermal management", Proc. of the Internat. Symposium on Advanced Packaging Materials: Process, Properties and Interfaces, March 11-14, 2001, pp. 360 - 365

[4] Beffort, S. Vaucher, F. A. Khalid, "On the Thermal and Chemical Stability of Diamond during Processing of Al/Diamond Composites by Liquid Metal Infiltration (Squeeze Casting)", Diamond and Related Materials 13 (2004), pp. 1834 - 1843.

[5] F. A. Khalid, O. Beffort, U. E. Klotz, B. A. Keller, P. Gasser, "Microstructure and Interfacial Characteristics of Aluminum-Diamond Composite Materials", Diamond and Related Materials 13 (2004), pp. 393 - 400

[6] Optigraph, http://www.optigraph.fta-berlin.de/optigraph.html, physical characteristics of high purity pyrolytic graphite published at http://www.optigraph.fta-berlin.de/basics.html (March 2006)

[7] S. Lee, "Optimum Design and Selection of Heat Sinks", IEEE Transactions on Components, Packaging, and Manufacturing Technology, Part A, Volume 18, Issue 4, Dec. 1995, pp. 812 - 817.

[8] U. Drofenik, G. Laimer, J. W. Kolar, "Theoretical Converter Power Density Limits for Forced Convection Cooling", Proceedings of the International PCIM Europe 2005 Conference, Nuremberg, Germany, June 7 - 9, pp. 608 - 619 (2005).

[9] U. Drofenik, G. Laimer, J. W. Kolar, "Pump Characteristic Based Optimization of a Direct Water Cooling System for a 10kW/500kHz Vienna Rectifier", IEEE Transactions on Power Electronics, vol. 20, no. 3, pp. 704-714, May 2005.

[10] H. D. Baehr, and K. Stephan, "Wärme- und Stoffübertragung", ISBN 3-540-64458-X, 3rd edition, Springer-Verlag (1998).

[11] Sanyo Denki Co., Ltd., http://www.sanyodenki.co.jp/, Webcatalog, Cooling Fan and CPU-Cooler, DC-Fan, datasheets published at http://sanyodb.colle.co.jp/product_db_e/coolingfan/dcfan/cooling_dcfan.html (March 2006)

[12] S. L. Dixon, "Fluid Mechanics and Thermodynamics of Turbomachinery", ISBN 0-7506-7059-2, Butterworth-Heinemann, 4th edition (1998).

[13] M. F. Holahan, "Fins, Fans, and Form: Volumetric Limits to Air-Side Heatsink Performance", IEEE Trans. on Components and Packaging Technologies, vol. 28, Issue 2, June 2005, pp. 255-262.